

## Boise State University ScholarWorks

---

Materials Science and Engineering Faculty  
Publications and Presentations

Department of Materials Science and Engineering

---

1-1-2017

# Signal-to-Noise Ratio Enhancement Using Graphene-Based Passive Microelectrode Arrays

Sepideh Rastegar  
*Boise State University*

Justin Stadlbauer  
*Boise State University*

Kiyo Fujimoto  
*Boise State University*

Kari McLaughlin  
*Boise State University*

David Estrada  
*Boise State University*

*See next page for additional authors*

---

**Authors**

Sepideh Rastegar, Justin Stadlbauer, Kiyo Fujimoto, Kari McLaughlin, David Estrada, and Kurtis D. Cantley

# Signal-to-Noise Ratio Enhancement Using Graphene-Based Passive Microelectrode Arrays

Sepideh Rastegar<sup>a),1</sup>, Justin Stadlbauer<sup>1</sup>, Kiyo Fujimoto<sup>2</sup>, Kari McLaughlin<sup>2</sup>, David Estrada<sup>2</sup>, and Kurtis D. Cantley<sup>b),1</sup>

<sup>1</sup>Department of Electrical and Computer Engineering and <sup>2</sup>Micron School of Materials Science and Engineering  
Boise State University, Boise, ID, USA

Email: <sup>a)</sup>sepidehrastegar@boisestate.edu, <sup>b)</sup>kurtiscantley@boisestate.edu

**Abstract**—This work is aimed toward the goal of investigating the influence of different materials on the signal-to-noise ratio (SNR) of passive neural microelectrode arrays (MEAs). Noise reduction is one factor that can substantially improve neural interface performance. The MEAs are fabricated using gold, indium tin oxide (ITO), and chemical vapor deposited (CVD) graphene. 3D-printed Nylon reservoirs are then adhered to the glass substrates with identical MEA patterns. Reservoirs are filled equally with a fluid that is commonly used for neuronal cell culture. Signal is applied to glass micropipettes immersed in the solution, and response is measured on an oscilloscope from a microprobe placed on the contact pad external to the reservoir. The time domain response signal is transformed into a frequency spectrum, and SNR is calculated from the ratio of power spectral density of the signal to the power spectral density of baseline noise at the frequency of the applied signal. We observed as the magnitude or the frequency of the input voltage signal gets larger, graphene-based MEAs increase the signal-to-noise ratio significantly compared to MEAs made of ITO and gold. This result indicates that graphene provides a better interface with the electrolyte solution and could lead to better performance in neural hybrid systems for *in vitro* investigations of neural processes.

**Keywords**—Neural interface; Microelectrode Arrays; Signal-to-noise ratio; CVD graphene; Noise power spectrum

## I. INTRODUCTION

Electronics that interface with the human body are becoming more prevalent and find potential application in areas such as brain-machine interfaces (BMIs), neuroscience and other types of medical research, and medical diagnostics. In order to translate bio-interface electronics into the clinical setting, fine tuning device performance is a current issue [1]. Microelectrode arrays (MEAs) have been rapidly gaining interest because they are able to electrically stimulate neuronal cells *in vitro* and *in vivo*. Additionally, they can be used to easily record the activity of cells at multiple points without rupturing them, in contrast to patch clamp techniques which cannot be used for long duration and are limited to a single cell measurements [2-5].

In electronics, noise is defined as a purely random fluctuation in an electrical signal, the instantaneous value or phase of the waveform cannot be predicted at any time [6, 7]. This is highly problematic in bioelectronics and neural interfaces and can severely degrade the precision of cellular measurements [8]. To overcome this problem, finding materials which can provide the

best possible signal integrity to an external recording device or amplifier circuit is critical. Subsequently reducing the noise and increasing overall SNR and is of great interest [9,10].

For decades various MEAs have been developed through novel techniques to record intracellular and extracellular activities of neuron cells. Since they are in direct contact with tissues, the biocompatibility of the MEAs is necessary. Metal based MEAs such as gold, platinum and iridium as well as polymer-based MEAs are considered non-toxic and are widely used in neural interface devices [11-15]. Promising results have also been obtained from optical transparent materials such as indium tin oxide (ITO) electrodes [16,17]. In addition to the materials mentioned above, using organic two-dimensional materials such as graphene in MEAs has been gaining interest. Graphene consists of a single atomic sheet of carbon and is one of the most promising materials for the next generation of MEAs. This is not only because of its biocompatibility with neuron cells, but also due to its high conductance and high mechanical strength [18-20]. In this work, SNR of graphene-based MEAs is compared with that of ITO and gold. The next section describes the fabrication of microelectrode arrays, and experimental set up is discussed in section III. Results are presented in section IV and finally conclusions are discussed in section V.

## II. MICROELECTRODE FABRICATION

### A. Indium-Tin-Oxide (ITO) MEA Fabrication

The ITO microelectrode arrays were fabricated on ITO coated glass obtained from Delta Technologies. The thickness of the ITO glass was 1.1 mm with the sheet resistance of 8–12  $\Omega$ /square. First, a 10 nm Cr layer was deposited using an AJA Orion sputter tool with the base pressure of 2.3  $\mu$ Torr, and DC power of 100 W for 108 seconds. The role of this layer is to help with the adhesion of Au layer, which is deposited right after Cr with base pressure of 1.7  $\mu$ Torr, and the DC power of 300 W for 75 seconds to get a thickness of 60 nm. Then, SPR220-3 photoresist was spin-coated onto the sample and soft baked on a hot plate at 115  $^{\circ}$ C for 90 seconds. The sample was then exposed for 15 seconds using a Quintel Q-4000 contact printer with lamp intensity of 15 mW/cm<sup>2</sup>. To define the pattern, the sample was immersed in MF26-A developer for 40 seconds and then hard baked at 115  $^{\circ}$ C on the hot plate for 10 minutes to be ready for further etching processes. First, the Au layer was etched for 1 minute using gold etchant ordered from VWR. Next, the Cr layer was etched using Cr etchant until the glass substrate became visible. Finally, the ITO layer was etched using diluted

This work was supported in part by the IDeA Network of Biomedical Research Excellence (INBRE) and the Center of Biomedical Research Excellence (COBRE) at Boise State under grants numbers P20GM103408 and P20GM109095 from the National Institutes of Health.

HCl (one part 37% HCl to three parts deionized water). The photoresist layer was removed by acetone sonication. For patterning gold contact pads, a second layer of photoresist was patterned with the same photolithography process as mentioned above and the Au etching and Cr etching was followed after that. The process was finalized by a photoresist strip step followed by an ashing step with oxygen plasma for 2 minutes at 50 W power. This helps remove any remaining residue from the sample surface. Top and cross-sectional views of the ITO MEAs are illustrated in Fig. 1.

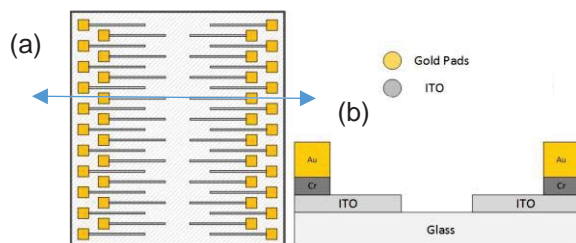


Fig. 1. (a) Top view illustration of the patterned ITO glass with gold contact pads. (b) Cross-section of the sample in part (a) at the position indicated.

## B. Graphene MEA Fabrication

The graphene microelectrode arrays were fabricated on plain Corning 1737 glass. First a 10 nm Cr layer was deposited using the AJA sputter tool with the base pressure of 2.3  $\mu$ Torr, and DC power of 100 W for 108 seconds to help the adhesion of 60 nm Au layer which is being deposited right after Cr deposition with the base pressure of 1.7  $\mu$ Torr, and the DC power of 300 W for 75 seconds. The same photolithography process as the ITO samples was used, but the Cr layer was etched for a few seconds using Cr etchant right after the Au layer etching using Au etchant for 1 minute. The photoresist layer was removed by acetone sonication and oxygen plasma ashing was done for 2 minutes at 50 W. Then, the CVD graphene was transferred onto the sample. For patterning the graphene MEAs, a second layer of photoresist is patterned with the same photolithography process as mentioned above and the graphene is etched using oxygen plasma at the power of 100W for 1 minute.

An in-house built low-pressure chemical vapor deposition (CVD) system was used for all graphene growth (1" quartz tube, lindberg/Blue M Mini-Mite Tube Furnace). HCl (37% Cleanroom LP, KMG Electronic Chemicals), Methane (10% Bal Argon Cert Std, UHP Gr P10, Norco), Argon (UHP grade, Norco), Hydrogen (>99.999% UHP grade, Norco), PMMA (495K A2 and 950K A4, anisole base solvent, 2% wt. and 4% wt., MicroChem), copper film (0.025 mm, annealed, uncoated, 99.8% metals basis), FeCl<sub>3</sub> (Copper etch type CE-100, Chemtrec), H<sub>2</sub>O<sub>2</sub> (30% Gigabit, KMG Electronic Chemicals) and acetone (ACS grade, Fisher chemical) were used without further purification. Raman spectroscopy was performed with a LabRAM HR Raman microscope with a 532 nm laser excitation to verify graphene quality.

### B.1 Chemical Vapor Deposition of Graphene on Copper

The procedure for chemical vapor deposition was adapted from a previously reported method by Ruoff [21]. Pre-cleaning of a 2 x 3" piece of copper film occurred by submerging the film

in a 1 M HCl bath for 3 min. Any remaining HCl was removed with nanopure H<sub>2</sub>O and the film was carefully dried with N<sub>2</sub>. Next, the copper film was rolled to the diameter of the quartz tube, and placed within the furnace. Annealing and growth steps occurred within the CVD system at 1 torr pressure. The copper foil was annealed at 1000 °C for 90 minutes under argon (100 SCCM) and hydrogen (100 SCCM) with a pressure of 1 torr. Graphene was grown for 75 minutes at 1000 °C facilitated with the use of methane (850 SCCM) and hydrogen (50 SCCM) gases. Finally, the samples were cooled under Ar (500 SCCM), and brought to atmospheric pressure.

### B.2 Poly(methyl methacrylate) (PMMA) Transfer

The procedure for graphene transfer was adapted from a previously reported method by Richter [22]. The graphene/copper (gr/Cu) was then cut to size (1x1") and gently flattened. Next, two layers of PMMA were drop coated onto the gr/Cu with an initial layer consisted of the 495 K A2 followed by 950 K A4. Each layer was cured at 200 °C for 2 minutes. The non-PMMA coated side (backside) of the gr/Cu film was exposed to an 1:1:20 HCl:H<sub>2</sub>O<sub>2</sub>:H<sub>2</sub>O solution for 10 minutes. Any excess solution was rinsed with nanopure H<sub>2</sub>O, and the backside was gently wiped down with acetone and rinsed with nanopure H<sub>2</sub>O. Gr/Cu was placed in a FeCl<sub>3</sub> solution at 60 °C for 4 hours. Subsequent rinsing of the gr/cu was performed before placing in a 1:1:20 HCl:H<sub>2</sub>O<sub>2</sub>:H<sub>2</sub>O solution for 10 minutes. Finally, the PMMA/gr was rinsed with nanopure H<sub>2</sub>O before transferring to the glass substrate. PMMA was removed with an 80 °C vapor bath (~10 hours), and any visible remaining residues were removed further with acetone dissolution.

### C. Gold MEA Fabrication

Gold MEAs were also fabricated on Corning 1737 glass. First a 10 nm Cr layer was deposited using AJA sputter tool with the base pressure of 2.3  $\mu$ Torr, and DC power of 100 W for 108 seconds to help the adhesion of 60 nm Au layer which is being deposited right after Cr deposition with the base pressure of 1.7  $\mu$ Torr, and the DC power of 300 W for 75 seconds. Then, the same photolithography process outlined previously was used to define the patterns. The Au layer was etched for 1 minute using gold etchant ordered from VWR. Then, the Cr layer was etched for a few seconds using Cr etchant such that the glass substrate is visible. The photoresist layer was then removed by acetone sonication followed by an ashing step with oxygen plasma for 2 minutes at 50 W power to make sure all the residue has been removed. An optical microscope image of the fabricated gold MEAs are shown in Fig. 2. This figure illustrates three different patterns of gold MEAs.

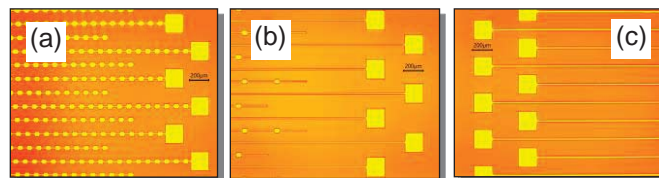


Fig. 2. Optical microscope images of the gold MEAs. (a) Pad chain pattern with pad spacing of 100  $\mu$ m. (b) Pad chains with pad spacing 200  $\mu$ m, and (c) line pattern. All the measurements in this work is done using the line pattern.

### III. EXPERIMENTAL SET UP

A 3D-printed nylon reservoir was mounted on the fabricated MEAs with the use of EASYPOXY K-230 from CYTEC such that the gold pads were located out of the reservoir so that the probe can be in direct contact with pads (Fig. 3). The reservoir was then filled with 1 mL of Dulbecco's Modified Eagle's Medium (DMEM, Corning, obtained from VWR) which is a neuron cell culture media. The sample was then placed on the chuck of an electrophysiology and semiconductor measurement probe station. A glass micropipette was pulled from filamentless borosilicate glass tubes with 1.5 mm outer diameter and 0.86 mm inner diameter (Sutter Instruments) using a Narishige PC-10 pipette puller. The micropipette was filled with the same solution used in reservoir using a syringe. The micropipette was then immersed in the electrolyte solution and kept 45  $\mu\text{m}$  above the microelectrode array (measured using the micrometer on the headstage). A Multiclamp 700B amplifier from Molecular Devices with CV-7B head stages was used to apply sinusoidal voltage signals with varying amplitudes and frequencies to the micropipette for each electrode material. Voltage signal response is measured with respect to the grounded external contact by a probe connected to an oscilloscope. Finally, a conversion of voltage to current is done based on the headstage circuit. In electrophysiology, voltage clamp involves applying a voltage (input) and observing the current response (output). The voltage clamp gain is calculated in equation (1).

$$\text{Gain} = \frac{V_{out}}{I_{in}} = \frac{0.5 \text{ V}}{1 \text{ nA}} = 0.5 \text{ V/nA} \quad (1)$$

Comparison of the measured signal relative to the average baseline noise enables calculation of the signal-to-noise ratio (SNR). A Fourier transform of DC current versus time, averaged over multiple measurement windows, provides a baseline noise-power spectrum [6].

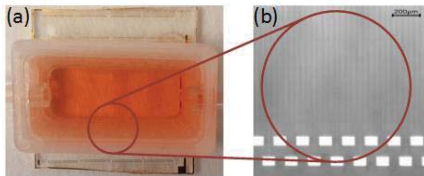


Fig. 3. (a) Photograph of the full patterned ITO passive microelectrode sample with a 3D-printed nylon reservoir adhered to the substrate and filled with 1 mL of DMEM solution. (b) Optical microscope image of zoomed ITO microelectrode arrays (MEAs) with gold contact pads.

### IV. RESULTS

Fig. 4a illustrates the applied input voltage signal with the frequency of 100 Hz and 1 mV amplitude of (2 mV peak-to-peak) versus time. First, a zero volt signal is applied to each of electrode materials and the current response in time domain is recorded (Fig. 4b)). This current indicates the DC noise coming from the substrate. The frequency spectrum of the DC noise current is obtained by calculating the Fast Fourier Transform (FFT) in MATLAB (Fig. 4c). Then, a 100 Hz input voltage signal with the amplitude of 1 mV is applied to the ITO MEAs and the frequency spectrum of the time domain current is obtained. (Fig. 4d). The same experiment is repeated with gold-

based MEAs and graphene-based MEAs and the results are illustrated in Figs. 4e and 4f, respectively. Sinusoidal signals of varying frequencies and amplitudes are applied to all three MEA materials and the SNR is calculated for each point. The SNR is then plotted versus the signal frequency and the signal amplitude. The results are discussed in following subsections.

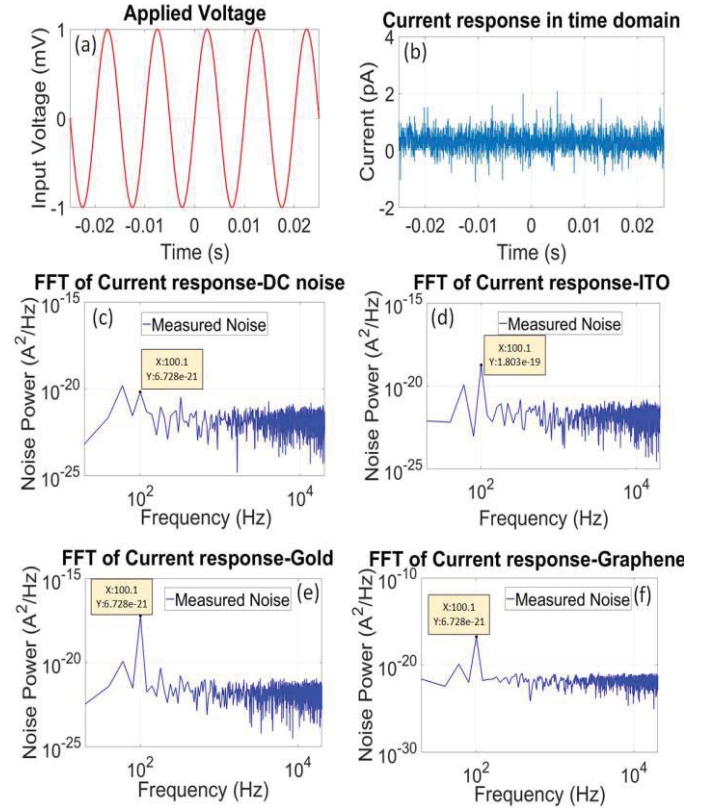


Fig. 4. (a) 100 Hz voltage signal with 1 mV amplitude which is applied to the glass micropipette. (b) Time domain current response when zero volts applied. (c) frequency spectrum of the current in part (b). (d) – (f) FFT of measured current response to voltage applied in part (a) for ITO, gold, and graphene MEAs respectively.

#### A. SNR vs Applied Signal Frequency

The frequency representation of a time signal is known as a “spectrum”. Power spectrum analysis is utilized in this section to characterize solution-based signal noise. The following can be used to calculate the signal-to-noise (SNR) ratio:

$$\text{SNR}(f) = \frac{P_S(f)}{P_N(f)} \quad (2)$$

In the above equation,  $P_S(f)$  is the power spectral density of the signal which is the Root Mean Square (RMS) of the measured current and  $P_N(f)$  is the power spectral density of noise and is named as the noise RMS value. Dividing the signal power by the noise power provides the SNR. In Fig. 5, input voltage signals with the amplitude of 2.5 mV and varied frequencies from 100 Hz to 1 kHz are applied to graphene, gold, and ITO MEAs and their SNR is compared. This result illustrates the noticeably higher SNR of graphene-based MEAs for the entire frequency range of 100 Hz to 1 kHz (chosen for the approximate bandwidth of action potentials). As the frequency gets higher, graphene appears to further outperform gold and ITO.

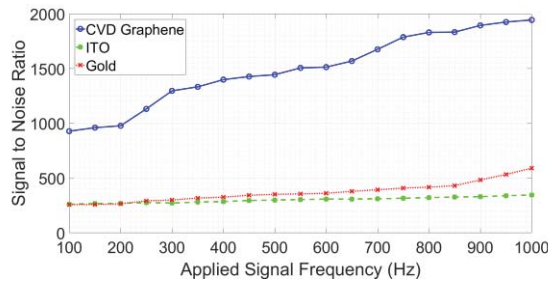


Fig. 5. Signal-to-noise ratio (SNR) of CVD graphene, gold, and ITO MEAs versus the frequency of the applied sinusoidal signal.

### B. SNR versus Applied Signal Amplitude

In Fig. 6, input voltage signals with the frequency of 100 Hz and varied amplitudes from 0.1 mV to 5 mV are applied and the SNR of three different materials is compared. This result proves that graphene significantly enhanced the SNR and as the magnitude of the applied voltage gets greater, the SNR of graphene-based microelectrodes increases remarkably compared to gold and ITO MEAs.

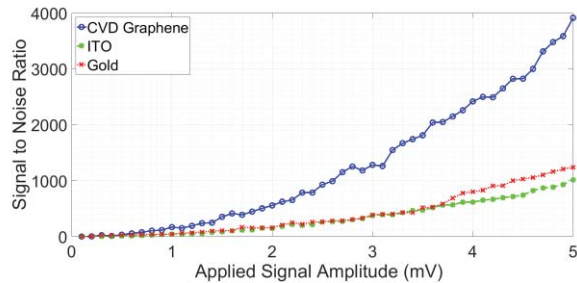


Fig. 6. SNR of CVD graphene, gold, and ITO MEAs versus the amplitude of the applied sinusoidal signal. The signal amplitude is varied from 0.1 mV to 5 mV and SNR is calculated at each point for each material.

## V. CONCLUSIONS

In this work, we fabricated neural microelectrode arrays (MEAs) using three different materials such as gold, ITO, and CVD graphene. Then, we applied voltages with varied frequencies and amplitudes to the fabricated glass micropipette which was immersed in an extracellular solution. Then, using a gold probe, we measured the output current response. The frequency spectrum was then obtained at each measuring point and the SNR was calculated by dividing the power spectral density of the signal by the power spectral density of noise. Comparing the SNR of all three MEA materials, we found that the graphene based microelectrode arrays significantly increased the SNR. This indicates that two-dimensional nanomaterials such as graphene may be an excellent candidate for measuring the activity of electrogenic cells in the future.

## REFERENCES

- [1] J. C. Kao, P. Nuyujukian, S. I. Ryu, M. M. Churchland, J. P. Cunningham, and K. V. Shenoy, "Single-trial dynamics of motor cortex and their applications to brain-machine interfaces," pp. 1–11.
- [2] Jimbo, Y., Kawana, A.: Electrical-stimulation and recording from cultured neurons using a planar electrode array. *Bioelectrochem. Bioenerg.* 29(2), 193–204 (1992). doi:10.1016/0302-4598(92)80067-Q
- [3] X.W. Du, L. Wu, J. Cheng, S.L. Huang, Q. Cai, Q.H. Jin, et al. Graphene microelectrode arrays for neural activity detection *J. Biol. Phys.*, 41 (2015), pp. 339–347

- [4] M. Heim, L. Rousseau, S. Reculosa, V. Urbanova, C. Mazzocco, S. Joucla, *et al.* Combined macro-/mesoporous microelectrode arrays for low-noise extracellular recording of neural networks *J Neurophysiol*, 108 (2012), pp. 1793–1803
- [5] U. Egert, B. Schlosshauer, S. Fennrich, W. Nisch, M. Fejt, T. Knott, *et al.* A novel organotypic long-term culture of the rat hippocampus on substrate-integrated multielectrode arrays *Brain Res. Protocols*, 2 (1998), pp. 229–242
- [6] K. D. Cantley, P. G. Fernandes, M. Zhao, H. J. Stiegler, R. A. Chapman and E. M. Vogel, "Noise Effects in Field-Effect Transistor Biological Sensor Detection Circuits," *IEEE Conference Publications*, pp. 370–373, 2012.
- [7] B. Carter, "Op Amp Noise Theory and Applications," in *Op Amps for Everyone*, Dallas, Texas Instruments, 2008, pp. 24–48.
- [8] Hai, A., Shappir, J. & Spira, M. E. Long-term, multisite, parallel, in-cell recording and stimulation by an array of extracellular microelectrodes. *J. Neurophysiol.* 104, 559–568 (2010).
- [9] Fromherz P, Offenhauser A, Vetter T, Weis J. A neuron-silicon junction: a Retzius cell of the leech on an insulated-gate field-effect transistor. *Science* 252: 1290–1293, 1991.
- [10] Fromherz P. Three levels of neuroelectronic interfacing: silicon chips with ion channels, nerve cells, and brain tissue. *Ann NY Acad Sci* 1093: 143–160, 2006
- [11] G. Marton, G. Orban, M. Kiss, R. Fiath, A. Pongracz, I. Ulbert, A multimodal, SU-8-Platinum – polyimide microelectrode array for chronic *In vivo* neurophysiology, *PLoS One* 10 (2015) 1–16
- [12] Gergely Márton, Gábor Orbán, Marcell Kiss, Richárd Fiáth, Anita Pongrácz, István Ulbert, K.D. Wise, et al., A multimodal, SU-8 – platinum – polyimide microelectrode array for chronic *in vivo* neurophysiology. Edited by Liset Menendez De La Prida, *PLoS One* 10 (12) (2015) e0145307, <http://dx.doi.org/10.1371/journal.pone.0145307> (Public Library of Science).
- [13] Kotzar G, Freas M, Abel P, Fleischman A, Roy S, Zorman C, et al. Evaluation of MEMS materials of construction for implantable medical devices. *Biomaterials.* 2002;23(13):2737–50. doi: 10.1016/S0142-9612(02)00007-8. pmid:12059024
- [14] Dymond AM, Kaechele LE, Jurist JM, Crandall PH. Brain tissue reaction to some chronically implanted metals. *J Neurosurg.* 1970;33(5):574–80. pmid:5479495
- [15] Ereifej E, Khan S, Newaz G, Zhang J, Auner G, VandeVord P. Comparative assessment of iridium oxide and platinum alloy wires using an *in vitro* glial scar assay. *Biomedical Microdevices.* 2013;15(6):917–24. doi: 10.1007/s10544-013-9780-x. pmid:23764951
- [16] Gross GW, Rhoades BK, Reust DL, Schwalm FU. Stimulation of monolayer networks in culture through thin-film indium-tin oxide recording electrodes. *J. Neurosci. Meth.* 1993;50(2):131–143. doi: 10.1016/0165-0270(93)90001-8
- [17] Park D-W, Schendel AA, Mikal S, Brodnick SK, Richner TJ, Ness JP, Hayat MR, Atry F, Frye ST, Pashaie R, Thongpang S, Ma Z, Williams JC. Graphene-based carbon-layered electrode array technology for neural imaging and optogenetic applications. *Nat. Commun.* 2014;5:5258. doi: 10.1038/ncomms6258
- [18] Geim, A.K., Novoselov, K.S.: The rise of graphene. *Nat. Mater.* 6(3), 183–191 (2007). doi:10.1038/Nmat1849
- [19] I.S. Jacobs and C.P. Bean, "Fine particles, thin films and exchange anisotropy," in *Magnetism*, vol. III, G.T. Rado and H. Suhl, Eds. New York: Academic, 1963, pp. 271–350.
- [20] Cheung KC. 2007. Implantable microscale neural interfaces. *Biomedical Microdevices* 9: 923–38
- [21] Li, X., Cai, W., Kim, S., Nah, J., Piner, R., Velamakann, A., Jung, I., Tutuc, E., Banerjee, S., Colombo, L., Ruoff, R. Large-area synthesis of high-quality and uniform graphene films on copper foils. *Science.*, 2009, 324, 1312–1314. DOI: 10.1126/science.1171245
- [22] Liang, X., Sperling, B.A., Calizo, I., Cheng, G., Hacker, C.A., Zhang, Q., Obeng, Y., Yan, K., Peng, H., Li, Q. and Zhu, X. Toward clean and crackless transfer of graphene. *ACS nano*, 2011, 5(11), 9144–9153.